Self-Mixing Interferometry for Biomedical Signals Sensing

Silvano Donati, *Life Fellow, IEEE*, and Michele Norgia, *Senior Member, IEEE*

(Invited Paper)

Abstract—**Self-mixing interferometry is a noncontact method well suited for measuring a variety of biological signals, like blood pressure wave at wrist and thorax (the optical stethoscope), blood velocity in vein and in external circulation, THz echoes from skin, ear drum vibration, and oculomotor reflex measurements. In this review, after presenting the underlying theory and the main developments of self-mixing, we analyze the applications to biosignal measurement reported so far, and illustrate potentialities and perspectives of the technique.**

Index Terms—**Optical interferometry, self-mixing interferometry, laser diodes, optical feedback.**

I. INTRODUCTION

THE self-mixing interferometer (SMI) is based on the feedback effect generated by a light illuminating a remote target and returning back into the laser cavity. It is almost 50 years since the first paper on SMI [1] has been published, just a few years after the discovery of the laser. Curiously, one of the applications anticipated in a textbook [2] for the laser interferometer was biomedical, that is, monitoring the blood pulsation (the optical stethoscope).

In the self-mixing process (see Fig. 1), a very minute fraction of the outgoing power P_0, say down to $1/A = 10^{-7}$–10^{-8}, already leads to measurable modulations of the cavity field, both in amplitude (AM) and in frequency (FM) [3]–[5]. The modulation indexes are equivalent to, and replace, the signals obtained in a conventional optical interferometer.

It is sufficient to detect the emitted power to observe the AM interferometric signal and be able to pick up information on amplitude and/or the phase of the returning field. For the pickup, we can use the monitor photodiode at the rear mirror of the laser, while on the front output of the laser we just need a collimating optics and eventually an attenuator to adjust the amplitude of the retuning signal.
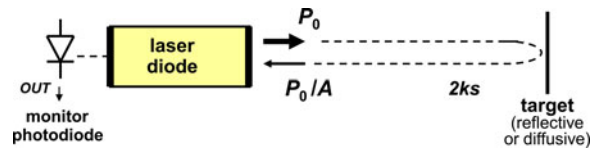
Fig. 1. Schematic of a self-mixing interferometer using a laser diode to sense the phase shift 2 ks of field returning from an external reflector (or diffuser) at a distance s.

Often, the target need not be reflective, as the weak back-diffused signal from a plain diffuser surface is large enough, up to a few meters distance. The only condition for a good SMI signal is that the laser is single longitudinal mode and has low side-mode content, as when it is biased well above threshold.

Because of the self-mixing process taking place in the cavity, the resulting power P deviates from the unperturbed power P_0 and can be written as [3], [5]:

$$P = P_0[1 + m_A F(\phi)] \quad (1)$$

where $\phi = 2ks$ is the optical phase shift suffered on propagation to the target and back, $k = 2\pi\lambda$ is the wavevector, and m_A is the AM modulation index, whose expression is found as [3]

$$m_A = A^{-1\backslash 2}[c/2 \; s(\gamma - 1/\tau)] \quad (2)$$

with $\gamma =$ gain per unit time of the medium and $\tau =$ cavity decay time. Here, the $-1/2$ dependence on power attenuation A shows how the SMI process depends on *field*, not *power*, and thus is a *coherent* process [3].

In (1), function F depends on the coupling strength, yet, it is always a 2π-periodic function of argument 2 ks, becoming the familiar cosine function for very weak coupling ($m_A \ll 1$). Thus, the F waveform swings over a full period as the target distance changes by $2 k\Delta s = 2\pi$. Solving for Δs, we get $\Delta s = \lambda/2$—just like in a plain interferometer.

We can introduce [5] an *injection parameter C* to describe the coupling strength as follows:

$$C = (1 + \alpha^2)^{1/2} \; A^{-1/2} \kappa \, s_0/n_{las}L_{las} \quad (3)$$

where κ is the fraction of field interacting with the laser mode, and α is the linewidth enhancement factor, s_0 is the target distance, n_{las} and L_{las} are the effective index of refraction and the cavity length of the laser, respectively.

The second modulation signal, FM, is found to affect frequency according to [3], [5], [6]

$$\omega = \omega_0[1 - m_F F(\phi\delta)] \qquad (4)$$

where $m_F = (c/2s_0) \, C/\omega_0$ is the FM modulation index, and $\delta = \text{atan} \, \alpha^{-1}$ is the phaseshift between AM (eq. 1) and FM.

For a He–Ne laser, α is close to zero and hence $\delta = \pi/2$. Working at weak coupling, the AM and FM signals are $F(\phi) = \cos\phi$ and $F(\phi + \delta) = \sin\phi$, respectively, and they constitute an orthogonal pair of functions that allows us to trace back unambiguously and measure the argument $\phi = 2 \, ks$.

This leads to the first class of an SMI instrument, i.e., the two-channel AM/FM based on the He–Ne laser source and capable of both vibration and displacement measurements. However, the FM signal cannot be measured directly because it is impressed upon the optical frequency ω_0, so we need to move it down to electrical frequency. This can be done in a He–Ne laser by Zeeman splitting the line so that two modes oscillate, one for SMI and the other serving as a local oscillator for down-conversion. Operation based on this principle has been demonstrated as early as 1978 [5], but in general its drawback is the rather complicated setup for the SMI source.

Going back to consider the waveform $F(\phi)$ of SMI signals, at weak coupling ($C < 0.01$) function F is a sine/cosine as in a normal interferometer, but as C is increased (from $C \approx 0.2$) the waveform becomes distorted [3]–[6] up to the critical condition $C = 1$ when a switching appears in the trailing edge (see Fig. 2). The regime of SMI with one switching per period is identified as *moderate coupling*, and is the second practical condition for SMI operation, called the 1-channel SMI.

At still increasing coupling, we find a second switching per period at $C = 4.6$ (see Fig. 2), and then ($C > 10$–30) many more additional switchings, up to the point that waveform becomes erratic, can jump on a multiple choice of switching. The laser now enters the regime of multistability and chaos [3], [4] which is no more useful for making measurements (rather, it is useful for chaos generators and secure transmission [7]).

The 1-channel SMI can be developed without incurring in the cosine ambiguity because the switching indicates the polarity of Δs increment, positive downward and negative upward. To operate the instrument, we just need to set the coupling strength C between 1.0 and 4.6.

With the 1-channel SMI, we can implement a digital measurement displacement, in multiples of $\lambda/2$-steps [8]–[10], and also, on locking at half fringe, a sub-nm amplitude measuring vibrometer [11], [12].

About the signal pickup, the most convenient to use is the rear output of the laser, as shown in Fig. 1, where the manufacturer usually provides a PD placed at a tilt angle for output power monitoring. Yet, if the rear PD is missing as in VCSEL or a QC laser, we can place a photodiode on the front output beam, and eventually detect the SMI signal at the target location [3]–[5]. Last, if PDs are not practicable, we can read the SMI signal as a (small) voltage superposed to the quiescent bias voltage [3], though the S/N ratio here is not as good as at the rear or front outputs.
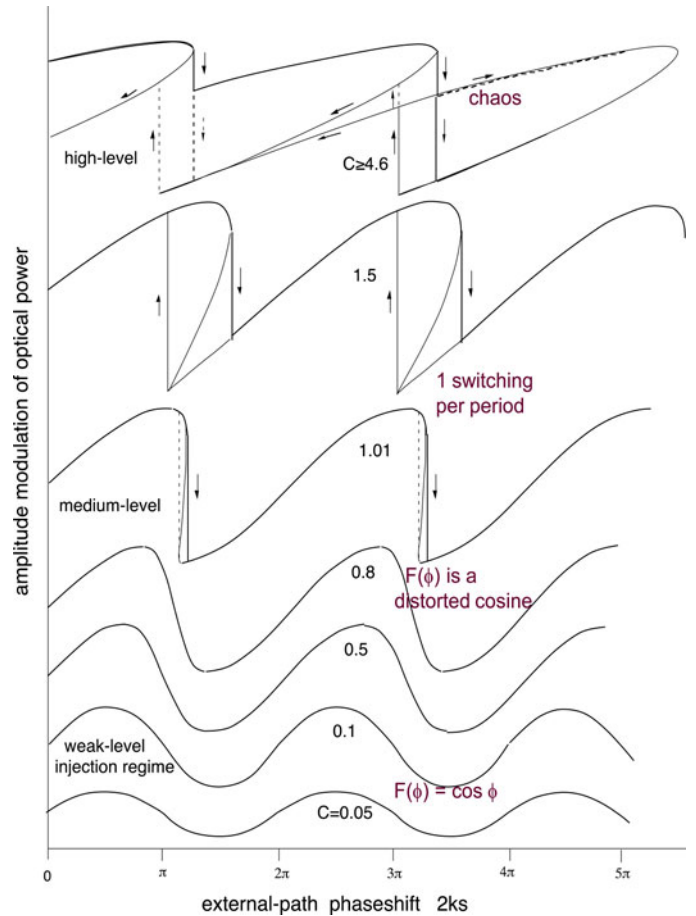

Fig. 2. At increasing coupling strength, the AM signal detected by the rear photodiode is initially ($C \ll 1$) a cosine function of pathlength $\phi = 2 \, ks$ like in a normal interferometer, then it becomes a distorted cosine ($C = 0.1$–0.9) up to $C = 1$ when it exhibits a switching, downward for increasing ϕ and upward for decreasing ϕ. At $C > 4.6$ the regime starts to become erratic with more than one switching per period.

II. FEATURES OF THE SMI INTERFEROMETER

From the user's point of view, when compared to common interferometric configurations, the 1-channel SMI has several intrinsic, advantageous features:

1) minimal part-count (we do not need any external optical interferometer);
2) setup is self-aligned (it measures where the laser spot falls);
3) no spatial, wavelength or stray-light filters are required (the Fabry–Perot cavity or DFB grating of the laser already acts as a filter);
4) can operate on a normal diffusing target surface [4], [10] (as the SMI tolerates a relatively strong loss A)—but then has to deal with speckle pattern statistics;
5) signal is everywhere on the beam, also at the target side (this feature is unique to SMI, and can be exploited in special applications);
6) resolution is $\lambda/2$ with fringe counting, and well below nanometers with analogue processing;
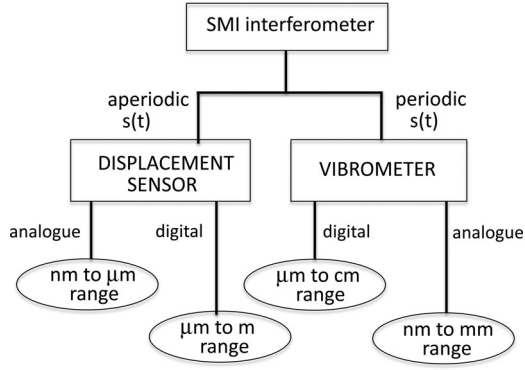
Fig. 3. Basic classification of SMI schemes, according to the $s(t)$ periodicity and the handling (analogue versus digital) of the electrical readout signal. The typical range (order of magnitude) usually covered is also indicated.
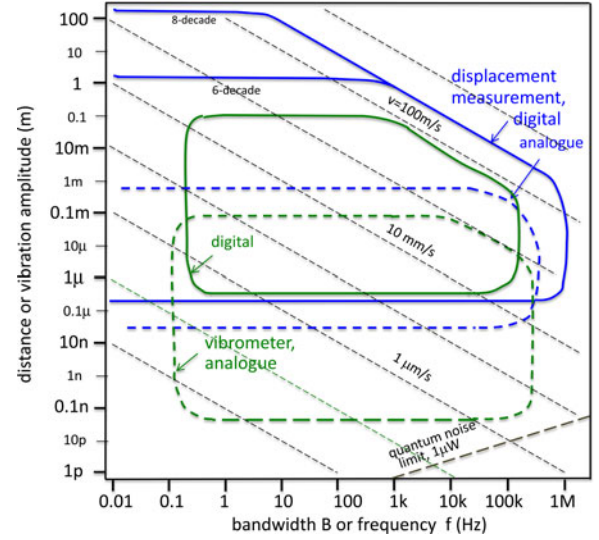

Fig. 4. Wegel's diagram of performance for displacement-measuring instruments and vibrometers. Amplitude of displacement is plotted versus bandwidth (or frequency of vibration) for digital and analogue handling of the signal. Upper limit of operation is set by dynamic range (or saturation effects), lower limit by noise (or discretization errors), left and right boundaries by frequency response of processing circuits; the $-45°$ slope limit is set by the Doppler-induced frequency content. The quantum noise theoretical limit for a detected power of $1\ \mu$W is also indicated.

7) quantum limit of detection easily approached, and minimum detectable displacement is $\ll \lambda$ (typ. $0.1-1\ \mathrm{pm}/\sqrt{\mathrm{Hz}}$).
8) bandwidth is easily up to hundreds kilohertz or megahertz

Of course, there are also disadvantages, like:

1) reference arm is missing (at least in the basic setup—but then we will be able to procure an electrical reference with the dual-SMI configuration [12]);
2) the transmitting optic is used also for collecting the return—this is a limitation in some applications;
3) long-term stability is poor with unexpensive Fabry–Perot LD (having $\Delta\lambda/\lambda < 10^{-3}$ or 3 digits); for metrology applications (calling 6 significant digits) we need a more expensive DFB [4], [8], [9];
4) flexibility is limited (as no reference arm is available).

For more details on SMI, we refer the reader to a recent review [4] illustrating the wealth of approaches to signal handling, and the corresponding rich variety of applications covered by SMI in several fields, from metrology to physical measurands, to biology.

III. TYPES OF SMI MEASUREMENTS

Usually, an interferometer is classified as a *displacement* measuring instrument, when we perform the measurement with a fraction of λ resolution over a large distance, for example up to a few meters, like in machine tool metrology and mechanical shop applications [3].

On the other hand, if we are interested to analyze periodic motions of small amplitude (typ. $1-100\ \mu$m peak to peak) as for vibration and mechanical fatigue analysis [3], [12], probably we will be using analogue processing, and the instrument is then called a *vibrometer*. Thus, we have the classification of SMI schemes depicted in Fig. 3.

About readout of phase $\phi = 2$ ks, we can make a digital processing of the output signal (see Fig. 1) supplied by the photodetector, $I_{\mathrm{ph}}(t) \propto I_{\mathrm{P-P}} \cos\phi$, by counting periods of the signal peak-to-peak swing $I_{\mathrm{P-P}}$, (or, the $\lambda/2$ variations Δs of target distance) [3], [8]–[10]. Or, we may use analogue processing for $I_{\mathrm{ph}}(t)$, because a small observed variation ΔI_{ph} corresponds to a small distance variation Δs, easily seen equal

to $\Delta s = (\lambda/2)\Delta I_{\mathrm{ph}}/I_{\mathrm{P-P}}$. Given that the minimum ΔI_{ph} we can appreciate with the analogue processing is much smaller than $I_{\mathrm{P-P}}$, resolution is much better than $\lambda/2$, reaching down to the nanometer easily, and with 20–50-pm attainable in experiments [11], [12] (see also Fig. 4).

The quantum noise limit of the minimum measurable AM is still smaller, (see [3]), down to $1-10\ \mathrm{fm}/\sqrt{\mathrm{Hz}}$ for mW-level detected signals.

At the opposite end, with digital processing of the $\lambda/2$-fringe-counts, the dynamic range (or, maximum displacement counted in $\lambda/2$-steps) is only limited by the number of decades we allocate to the counter, until we reach to the coherence length of the source [3], and it can readily attain 6–8 decades of $\lambda/2$ steps, opposite to just one half-wavelength (a $I_{\mathrm{P-P}}$ swing) of the analogue processing.

We can summarize the performance of the approaches as shown in Fig. 4, where the contours indicate the area of operation of typical commercial and laboratory instruments.

Another measurement developed with SMI is that of *echoes detector*, the measurement of (returning) field amplitude. Indeed, the SMI process is coherent, because it is the result of the sum of fields in the active cavity, and thus it easily attains the quantum noise limit [3] of detection. SMI can reach for amplitudes of detectable echoes as small as $10^{-8}-10^{-9}$ of the outgoing optical power [3], [13], [14], as illustrated in the example of Fig. 5.

A variant to the back-mirror photodiode usually employed in the SMI is using the output across the laser diode terminals [14]. This is especially interesting at THz frequency where we can dispense from using a photodiode.
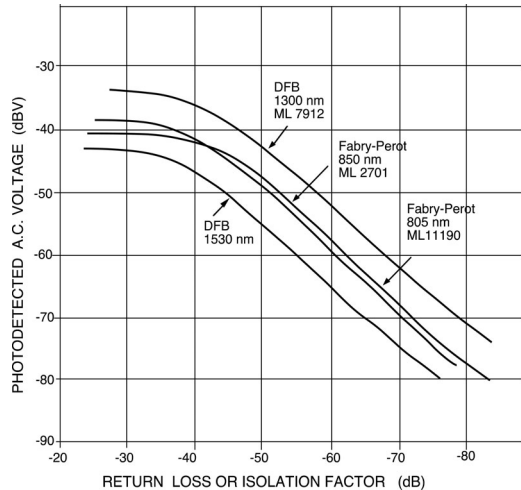
Fig. 5.   Typical signal amplitude obtained by an SMI as a response to a backreflected return in the laser cavity, as a function of attenuation respect to outgoing power. Responses of several different laser diodes are plotted. Upper limit is due to saturation of self-mixing signal, lower limit to noise (adapted from [3]).
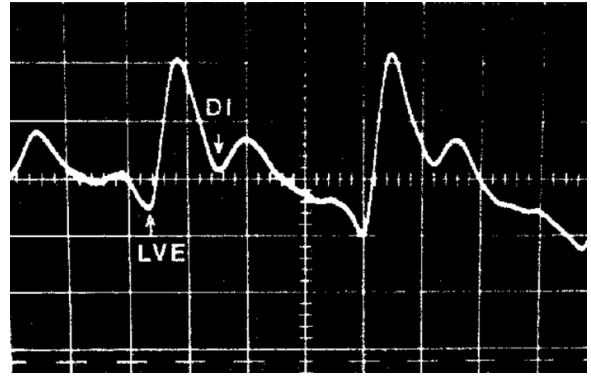

Fig. 6.   Blood pulsation waveform $s(t)$ measured on the finger tip with the two-channel analogue SMI reveals features usually found in a standard ECG, like LVE and DI. Vertical scale of displacement: 0.1 μm/div, horizontal scale 0.2 s/div (from [15]).

So, in general we may regard SMI as a probe to the optical echo signals returning back from a remote experiment external to the source.

In conclusion, the SMI is a sort of injection detection that can supply information not only on the *phase* of the returning signal (as in interferometry) but also on its *amplitude* (as an echo detector).

IV. SMI MEASUREMENTS OF BIOLOGICAL SIGNALS

A. Motility and Vibro-Cardiography

In an early experiment with two-channel He–Ne analogue SMI [15], we demonstrated that the SMI can pickup optically, without physical contact, several biological signals associated with motility, like the blood pulsation, respiratory sounds and tremor.

In particular, the blood pulsation on the finger tip of a normal subject was readily observed [15]. The detected waveform resembled a replica of the cardiac pulsation, and details like the left ventricular ejection (LVE) and dichrotic incisure (DI) were clearly recognized in it, see Fig. 6, the features of normal ECG well-known to the cardiologist.

Thus, the SMI technique, later called vibro-cardiographic (VCG) pickup, interestingly can supply information similar to electrocardiography (ECG) but without electrical connection nor any physical contact to the patient.

Additional measurements carried out with the two-channel analogue SMI were: respiratory sounds—revealing that spikes found with normal acoustical stethoscope and missing in the optical pickup are artifacts caused by skin slipping under the stethoscope—and tremor of hands due to nervous disorders.

After the first demonstrations, many researchers have continued the experiments with SMI, confirming the suitability of the methods and clarifying important details.

Hong and Fox [16] measured the blood-induced pressure wave by means of a conventional Michelson interferometer that

had one arm ending on a fiber tip to facilitate positioning. They found waveforms with general trends similar to Fig. 6, yet with number of spikes and shape details varying on different districts of the body, for example the perispheral arteries and the area of the tricuspid valve. They attributed the differences to reflections of the pressure wave, and suggested that the skin vibration profile (or VCG waveform) could be indicative of vascular elasticity. They were able to accurately measure delays in the range 0.05–0.3 s between the peaks of ECG and VCG in several districts of the body, thus allowing an evaluation of the pressure wave velocity, an index of arterial distensibility.

Using a 1-channel SMI laser-diode vibrometer, J. Hast *et al.* [17] measured the Doppler signal of the cardiovascolar pulse in radial arteries of the forearm. The Doppler signal is the time derivative of phase $d\phi/dt = 2\,kv$ associated with displacement $s(t)$ [see the waveform of Fig. 6]. They conducted a survey on a sample of 200 volunteers, and found that $d\phi/dt$ is well correlated (with a correlation degree $\chi = 0.84$) to the time derivative of the blood pressure waveform taken on peripherical district (the middle finger) with a conventional sensor. This is an important result confirming the validity of diagnostic made by SMI. Thus, pressure wave $P(t)$ and displacement $s(t)$ differ just for a constant.

Recently [18] Capelli *et al.* used an SMI vibrometer to detect the displacement $s(t)$ of the blood pressure wave in the wrist radial artery. Comparing the VCG to the normal ECG signal taken by a three-electrode placement (hip and hands) they again confirmed the good correlation of peak positions of the two traces, despite differences of fine details, and were able to measure pressure wave delays.

Another measurement with the two-channel He–Ne SMI was on respiratory sounds on the back of a patient (see Fig. 7).

Inspiration and expiration sounds were clearly measured, finding waveforms similar to those of the traditional acoustical stethoscope, except for missing spikes, identified as artifacts due to skin friction under the stethoscope during respiration [15].

Recently, a 1-channel SMI was used by Norgia and coworkers to measure the transfer impedance $Z_{\mathrm{tr}} = \Delta P/V$ of the respiratory system by a forced oscillation technique [21]. The transfer
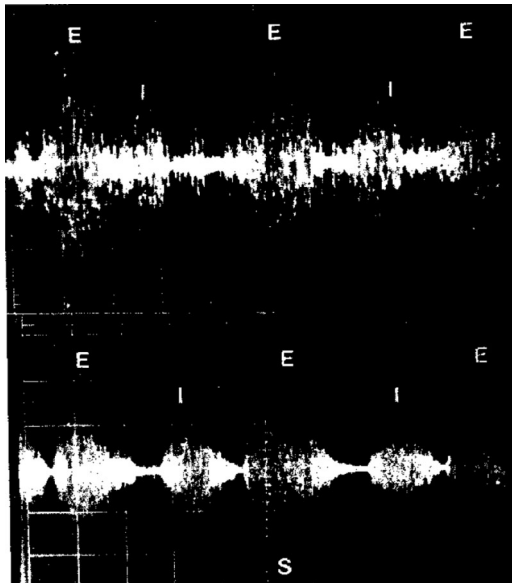
Fig. 7. Respiratory sound detected by (bottom) the two-channel analogue SMI and (top) by an acoustical stethoscope, on a few periods of inspiration (I) and expiration (E). Amplitude scale: 200 nm/div, time scale 0.75 s/div. Artifacts due to skin friction under the microphone are missing in the optical pickup (from [15]).
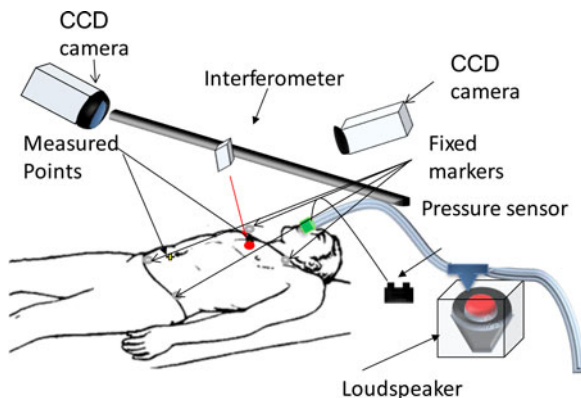

Fig. 8. Setup for measuring the thoraco-abdominal displacement by the 1-channel SMI. A loudspeaker produces the pressure stimulus, read by a pressure sensor at the mouth opening.

impedance provides informations on tissues and airways, and is useful for assessing the mechanical properties of lungs and associated disorder. To compute Z_{tr}, a breathing pressure variation ΔP was applied to the mouth of the patient by a loudspeaker (see Fig. 8) and the corresponding SMI waveform $S = \cos 2\, ks(t)$ induced on the thorax was measured. Then, displacement $s(t)$ was calculated from S by a new algorithm consisting of three steps: 1) finding the (unsigned) velocity $|v|$ by computing the signal FM content, $v = (\lambda/2)\, f_{SM}$, where f_{SM} is the local fringe FM of the SMI signal S; 2) finding the sign of velocity between two stationary points of waveform C, by an original algorithm applied to the signal derivative [21]; and 3) integrating v to obtain s.

An *in vitro* test of the system (see Fig. 9) has validated the measurement, showing that it attains a resolution down to λ and a dynamic range up to 10 mm.
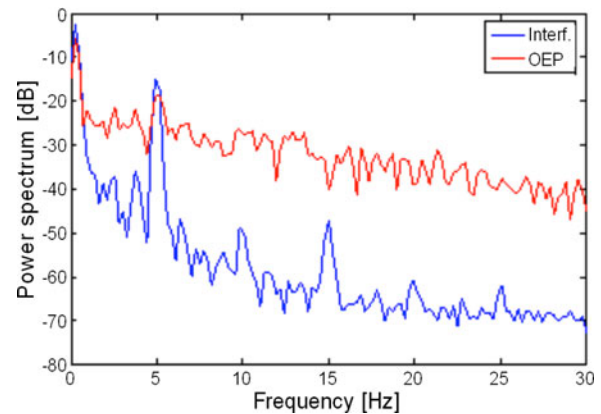

Fig. 9. Spectra of displacement at the sternum for a 5-Hz excitation as measured by the SMI (botom curve) and by a commercial optical motion analysis system (OEP). Sensitivity of SMI is at least 20–25 dB better than OEP.

Results of *in vivo* experiments [21] were in good agreement with a standard optoelectronic motion analysis system (OEP), but had a much better sensitivity (at least 20 dB higher).

Fig. 9 shows a comparison for a small stimulus at 5 Hz, measuring the displacement of the sternal angle.

B. Speckle Effects

In all the experiments of optical pickup by conventional or SMI interferometry, the skin surface need not be treated for increased reflectivity, given that the weak return from a diffuser at some tens of cm distance is generally large enough to make a measurement with good SNR [15], [17], [21].

However, the targeted area has to be immobilized to avoid corruption of SMI signals due to the speckle pattern statistics.

As it is well known [3], [24], the speckle pattern is the grainy appearance of the laser spot projected on a diffuser surface, and it is due to the random-walk process resulting from the addition of elemental field contributions randomized in phase by the diffusing surface roughness (on a scale $\gg \lambda$).

The speckle statistics is responsible of fluctuations of the SMI signal $E = E_0 \cos 2\, ks$ giving rise to: 1) *amplitude fading* (fluctuations of E_0), especially important in a 1-channel interferometer [3] and 2) *phase error* added to 2 ks [25].

While the phase error is small when the dynamic range of measurement Δs is small compared to the longitudinal speckle size [3], [25], amplitude fading is a serious source of impairment because it entails occasional loss of the SMI signal, both in digital (signal too small to trigger the counter discriminator) and analogue processing (signal affected by a serious scale factor error).

Amplitude fading can be mitigated by several remedies like: 1) using a superdiffusing target surface (signal increases by a factor 20–50); 2) adding an automatic gain control (AGC, recovering up to a factor 100 of amplitude fading); and also 3) by high-pass filtering (to remove the baseline drift).

In addition, two new techniques have been recently introduced that enhance the immunity to speckle effects: the bright speckle tracking (BST, see [10]) and the half-fringe locking (see [12]).

The former is based on the introduction of a small transversal beam deflection on the target, so as to control and maximize the speckle projected back into the laser and its AM: riding the bright speckles strongly reduces the probability of falling in a very weak one.

The latter is a revisiting of the half-fringe operation of the interferometer, now aided by a feedback loop that keeps the phase constant (at $\pi/4$ or half fringe) by acting on the wavelengh. Seen by the feedback loop, amplitude fluctuations are external perturbations and as such their effect is decreased by a factor equal to the loop gain plus one $(1 + \beta A)$ as well-known from control theory, or strongly reduced as we can make $\beta A \approx 500$ in practice.

Operation of the SMI on living tissues is satisfactory when one or more of the aforementioned methods is used, but of course we still need some immobilization of the target area to avoid incurring in a large drift (or motility artifact) superposed to the useful signal, that shall then be filtered out.

C. Blood Velocity

SMI techniques are ideally suited for measuring blood velocity, because the interferometric signal $S = \cos 2\,ks$ carries the velocity v as the frequency content associated to the signal, that is $f = \omega/2\pi = (1/2\pi)\, d\phi/dt = 2\,kv/2\pi = 2v/\lambda$.

Blood velocity diagnostics is potentially interesting for *in vivo* applications as well as for extracorporeal circulation monitoring.

In vivo applications require that we enter into the blood vessel with a needle carrying an optical fiber pigtail connected to the laser. The fiber shall be monomode to preserve the spatial coherence, and usually no additional optical element will be necessary external to the fiber to obtain a good self-mixing signal returning from blood cells. The only requirement is that the end faces of the fiber tip shall be antireflection coated and possibly slanted at 8–12° to avoid spurious returns from being added to the useful signal.

Another possible caveat is the multiple scattering regime generated by the optically thick medium we look through [19]. As an example, the effect of multiple scattering on velocity measurement through a Doppler system has been evaluated by J. Moger *et al*. [20]. To limit the associated phase noise and smearing of the Doppler peak, we can use a source with limited temporal coherence like an SLED (superluminescent light-emitting diode) and a double-return arrangement for the readout beam, as introduced in [21].

Using a superluminescent diode at 830 nm as the source of the SMI, Rovati *et al*. [21] were able to measure the velocity profile of a liquid flowing in a vein-simulating capillary tube. The Doppler-shifted frequency covered a range of frequency 5–70 kHz, and the corresponding measured velocity was from 20 to 250 mm/s. By scanning the spot focussed in the capillary, Rovati *et al*. also measured the parabolic velocity profile of the flow [21].

In another experiment, deMul *et al*. were able to measure the velocity of a fluid simulating human blood (water with dispersed polystyrene spheres), obtaining a response factor of $v/f = 0.455$ cm/s·Hz with a 780-nm Fabry–Perot LD [22]. They
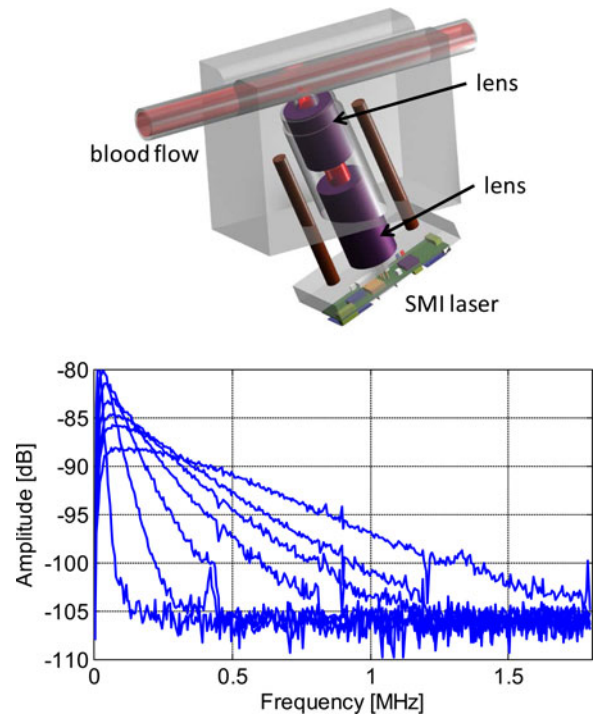

Fig. 10. Optical layout of the SMI laser to measure flux velocity, aimed to the capillary tube at a slant angle of 20° (top), and spectral distributions at different blood flows, 0.1, 0.5, 0.9, 1.3, 1.7, 2.1 and 3 L/min (bottom).

also succeeded in measuring the perfusion signal at a fingertip, a signal showing the heartbeat as the fundamental component and higher frequency for the blood flow.

Pesatori *et al*. [26] reported an improved version of the SMI for blood flow measurement, see Fig. 10, where the capillary tube used for extracorporal circulation is aimed axially at a slant angle θ to develop a signal $2v/\lambda \cos\theta$, allowing to cover the range of velocity from 5 to 65 cm/s, with a scale factor of 0.25 cm/s· Hz at $\lambda = 780$ nm.

In this study, optical scattering was also simulated, in order to elaborate the best signal processing for recovering the blood flow from the signal spectrum, and to find the system sensitivity to blood parameters.

Also a VCSEL laser diode can supply a good SMI signal from a scattering medium, and Nikolic *et al*. [27] have used it to measure the parabolic profile of velocity inside a capillary tube of 320-μm diameter, with a velocity ranging from 2 to 8.5 mm/s, and a standard deviation of about 1,5%.

An early experiment was carried out by Odzemir *et al*. [28] at a zero slant angle θ (i.e. looking the capillary at right angle) where no Doppler signal is expected (because $\cos\theta = 0$). Yet, they found again a frequency dependence of the returning signal amplitude, though noisy and dominated by the speckle statistics.

The velocity-dependent signal at $\theta = 0$ can be explained as generated by the speckles spots sliding under the field of view, at a (mean) frequency $f = v/s_t$, where $s_t = \lambda s/w_0$ is the transversal speckle size and w_0 is the laser spot size.

However, in this regime, the scale factor was much smaller than in the Doppler regime, typically $v/f = 0.8 \cdot 10^{-4}$ cm/s· Hz [28], [29], and this value represents what we can be assumed

as an estimate of speckle noise superposed and affecting the normal ($\theta \neq 0$) Doppler signal.

Taking advantage of the shorter emission wavelength of a GaN laser diode, $\lambda = 405$ nm, and using a slant angle $\theta = 15°$ to look at the capillary tube, R. Kliese *et al.* [30] were able to go down to as low as 26 μm/s as the minimum flow velocity measurable by the SMI.

In conclusion, SMI-based measurements of blood velocity and velocity profile have been validated by several Authors independently, and can be safely regarded a viable technique in biomedical instrumentation.

D. Echo Detector

As a detector of weak returns, the SMI has been employed [14] in the 3rd window of optical fibers to measure small optical signals and return losses [30]. The amplitude of detectable signal can be very small because the self-mixing process is coherent and the resulting output has a signal-to-noise ratio basically limited by quantum noise [3].

So, it is relatively easy to reach a sensitivity down to -80–-90 dB below the level of outgoing signal power, as demonstrated in the context of optical-isolator testing [13].

Recently, Dean *et al.* [31], have proposed SMI detection of T-waves. The application is about sensing with a quantum cascade THz laser, with the prospect of using it as an optical radar on living tissue target, to detect skin cancer.

In their experiment, they used the anode-to-cathode voltage of the laser diode as the output of the sensor, dispensing from the use of a detector. This mode of operation, called LV-SM (laser-diode voltage self-mixing) in contrast to the normally employed one, PD-SM (photodiode self-mixing) [14] is particularly attractive when the photodetector is unavailable or very noisy, like at THz frequency. Using a system (yet not optimized), Dean *et al.* obtained a sensitivity to weak return of -54 dBm, comparable to those of a good conventional detector [31]. Yet, a calculation has shown [14] that potentially we can reach the quantum limit at about -84 dBm.

The SMI sensor has been applied also to the confocal microscope, used to image biological tissues. Following Lu *et al.* [31], the use of SMI was found to greatly simplify the alignment of the optical setup.

In-depth resolution can reach 30–50-nm after an electronic processing of the SMI detected signal [32].

A scanning profilometer, based on a SMI confocal microscope, capable of resolving 10-nm height on sample of 5-mm by side demonstrated by Wang and Lay [33].

E. Ocular Reflex

The ocular reflex is a motility signal easily detected by the an SMI configured as a flow velocimeter.

Using a $P_0 = 1$-mW, $\lambda = 1550$-nm diode laser to comply with the laser safety standard of Class 1, Capelli and Giuliani [34] measured the speed of rotation of the eye in the range 0 to 500 deg/s, with a reported accuracy of 10% after averaging on a $N = 10$ measurements sample.

The ocular reflex is one component necessary to assess the vestibular reflex response, and is the companion measurement of the head rotation, which can be performed by means of an electrooptical gyroscope mounted on the head of the patient, as reported in details in [35].

V. CONCLUSION

We have outlined the principles of self-mixing interferometry and illustrated how it has become nowadays a mature technology, providing the researcher with an important tool for probing and measuring biomedical signals. Not only the many examples of success are remarkable, but also surprising is the variety of optical configurations and of signal processing that many Authors worldwide have successfully developed from the basic ideas.

Thus, we may conclude that SMI is opening the way to new and groundbreaking applications of biophotonics.

REFERENCES

[1] D. M. Clunie and N. H. Rock, "The laser feedback interferometer," *Rev. Sci. Instr.*, vol. 41, pp. 489–492, 1964.

[2] V. H. Steel, *Interferometry*. Cambridge, U.K.: Cambridge Univ. Press, 1967.

[3] S. Donati, *Electrooptical Instrumentation*. Upper Saddle River, NJ, USA: Prentice–Hall, 2004, Sec.4.5.2.

[4] S. Donati, "Developing self-mixing interferometry for instrumentation and measurements," *Laser Photon. Rev.*, vol. 6, pp. 393–417, 2012.

[5] S. Donati, "Laser interferometry by induced modulation of the cavity field," *J. Appl. Phy.*, vol. 49, pp. 495–497, 1978.

[6] S. Donati and M. Fathi, "Transition from short-to-long cavity and from self-mixing to chaos in a delayed optical feedback laser," *IEEE J. Quantum Electron.*, vol. 48, no. 10, pp. 1352–1359, Oct. 2012.

[7] S. Donati and S.-K. Hwang, "Chaos and high-level dynamics in coupled lasers and their applications," *Prog. Quantum Electron., 2012*, vol. 36, no. 2–3, pp. 293–341, Mar.–May 2012.

[8] S. Donati, G. Giuliani, and S. Merlo, "Laser diode feedback interferometer for measurement of displacement without ambiguity," *IEEE J. Quantum. Electron.*, vol. 31, no. 1, pp. 113–119, Jan. 1995.

[9] M. Norgia and S. Donati, "A displacement-measuring instrument utilizing self-mixing interferometry," *IEEE Trans. Instrum. Meas.*, vol. 52, no. 6, pp. 1765–1770, Dec. 2003.

[10] M. Norgia, S. Donati, and D. d'Alessandro, "Interferometric measurements of displacement on a diffusing target by a speckle-tracking technique," *IEEE J. Quant. Electr.*, vol. 37, no. 6, pp. 800–806, Jun. 2001.

[11] G. Giuliani, S. Bozzi-Pietra, and S. Donati, "Self-Mixing laser diode vibrometer," *Meas. Sci. Technol.*, vol. 14, pp. 24–32, 2003.

[12] S. Donati, M. Norgia, and G. Giuliani, "Self-mixing differential vibrometer based on electronic channel subtraction," *Appl. Opt.*, vol. 45, pp. 7264–7268, 2006.

[13] S. Donati and M. Sorel, "A phase-modulated feedback method for testing optical isolators assembled in the laser package," *IEEE Photonics Technol. Lett.*, vol. 8, no. 3, pp. 405–408, Mar. 1996.

[14] S. Donati, "Responsivity and noise of self-mixing photodetection schemes," *IEEE J. Quantum Electron.*, vol. 47, no. 11, pp. 1428–1433, Nov. 2011.

[15] S. Donati and V. Speziali, "Laser interferometry for sensing of respiratory sounds," in *Proc. Conf. Laser Electrooptics Appl.*, Washington, DC, USA, Jun. 1977, *Digest in IEEE J. Quant. Electr.*, vol. QE-13 (1977), pp. 798–87D, see also: "Interferometric Sensing of Respiratory Sounds," *Laser & Elektro-Optik* vol. 12, 1980, pp. 34–35.

[16] H. D. Hong and M. D. Fox, "No-Touch pulse measurement by optical interferometry," *IEEE Trans. Biomed. Eng.*, vol. 41, no. 11, pp. 1096–1098, Nov. 1994.

[17] J. Hast, R. Myllylä, H Sorvoja, and J. Miettinen, "Arterial pulse shape measurement using self-mixing effect in a diode laser," *IoP Quantum Electron*, vol. 32, pp. 975–982, 2002.

[18] G. Capelli, C. Bollati, and G. Giuliani, "Non-contact monitoring of heart beat using optical laser diode vibrocardiography," in *Proc. Biophoton.*, Parma, Italy, Jun. 8–10, 2011, pp. 1–3.

[19] V. V. Tuchin, *Tissue Optics: Light Sscattering Methods and Instruments for Medical Diagnosis*.   Washington, DC, USA: SPIE Press, 2007.

[20] J. Moger, S. J. Matcher, C. P. Winlove, and A. Shore, "The effect of multiple scattering on velocity profiles measured using Doppler OCT," *J. Phys. D: Appl. Phys.*, vol. 38, pp. 2597–260, 2005.

[21] L. Rovati, A. Cattini, and N. Palanisamy, "Measurement of the fluid-velocity profile using a selmixing superluminescent diode," *Meas. Sci. Techn.,*, vol. 22, 2011.

[22] F. F. M. deMul, M. H. Koelink, M. H. Weijers, J. G. Aarnoudse, R. Graaff, and A. C. Dassel, "Self-mixing laser-Doppler velocimetry of liquid flow and of blood perfusion in tissue," *App. Opt.*, vol. 31, pp. 5844–51, 1992.

[23] I. Milesi, M. Norgia, P. P. Pompilio, C. Svelto, and R. Dellacà, "Measurement of local chest wall displacement by a compact self-mixing laser interferometer," *IEEE Trans. Instrum. Meas.*, vol. 60, no. 8, pp. 2894–2901, Aug. 2011.

[24] J. W. Goodman, *Speckle Phenomena in Optics: Theory and Applications*. Greenwood Village, CO, USA: Roberts and Company Publ., 2007.

[25] S. Donati and G. Martini, "Speckle-Pattern intensity and phase second-order conditional statistics," *J. Opt. Soc. Amer.*, vol. 69, pp. 1690–1694, 1979.

[26] A. Pesatori, M. Norgia, and L. Rovati, "Self-Mixing laser doppler spectra of extracorporeal blood flow: A theoretical and experimental study," *IEEE Sensor J.*, vol. 11, no. 3, pp. 552–557, Mar. 2011, see also *Proc. Biophotonics 2011*.

[27] M. Nikolić, Y. L. Lim, S. J. Wilson, A. D. Rakić, L. Campagnolo, J. Perchoux, and T. Bosch, "Flow profile measurement in micro-channels using changes in laser junction voltage due to Self-mixing effect," in *Proc. IEEE Conf. Sensors*, Taipei, Taiwan, Oct. 28–31, 2011, pp. 259–262.

[28] S. K. Özdemir, S. Takamiya, S. Ito, S. Shinohara, and H. Yoshida, "Self-mixing laser speckle velocimeter for blood flow measurement," *IEEE Trans. Instrum. Meas.*, vol. 49, no. 5, pp. 1029–1035, Oct. 2000.

[29] S. K. Özdemir, I. Ono, and S. Shinohara, "Comparative study for the assessment of blood flow measurement using self-mixing speckle interferometry," *IEEE Trans. Instrum. Meas.*, vol. 57, no. 2, pp. 355–363, Feb. 2008.

[30] R. Kliese, Y. L. Lim, T. Bosch, and A. D. Rakić, "GaN laser self-mixing velocimeter for measuring slow flows," *Opt. Lett.*, vol. 35, pp. 814–816, 2010.

[31] P. Dean *et al.*, "Terahertz imaging through self-mixing in a quantum cascade laser," *Opt. Lett.*, vol. 36, pp. 2587–2589, 2011.

[32] C.-H. Lu, J. Wang, and K.-L. Deng, "Imaging and profiling surface micro-structures with noninterferometric laser feedback," *Appl. Phys. Lett.*, vol. 66, pp. 2022–2024, 1995.

[33] M. Wang and G. Lai, "Self-mixing microscopic interferometer for the measurement of microprofile," *Opt. Commun.*, vol. 238, pp. 237–244, 2004.

[34] G. Capelli and G. Giuliani, "Laser velocimeter for the measurement of eye movements," in *Proc. Biophoton.*, Jun. 8–10, 2011, paper Fr4.3.

[35] S. Donati, V. Annovazzi Lodi, L. Bottazzi, and D. Zambarbieri, "Pickup of head movement in vestibular reflex experiments with an optical fiber gyroscope," *IEEE J. Selected Topics Quantum Electron.*, vol. 2, no. 4, pp. 890–894, Sep.-Dec. 1996.

Silvano Donati (M'75–SM'98–F'03–LF'09) received the Doctor in Physics degree (Laurea in Fisica) from the University of Milan, Milan, Italy, in 1966. He is currently a Visiting Professor at National Chung-Hsing University, Taichung, Taiwan, and also a Lecturer in Optoelectronics at the Faculty of Engineering, University of Pavia, Italy, where he has been a Chair professor from 1980 to 2010. He has authored or coauthored about 300 papers and holds a dozen patents. He has introduced self-mixing interferometry and chaos-shift-keying cryptography, the topics covered in his Distinguished Lecture talk given in 21 LEOS (now IPS) Chapters in two terms, 2007/08 and 2008/09. He is the author of two books, *Photodetectors* (Prentice Hall, 1999) and *ElectroOptical Instrumentation* (Prentice Hall, 2004) the latter translated into Chinese (Jiao Tong University Press). He was the founder (1996) and first Chairman (1997–2001) of the Italian LEOS Chapter, LEOS VP Region 8 Membership (2002–04), LEOS Board of Governors Elected member (2004–06), and Chairman of the IEEE Italy Section (2008–09). He acted as a Guest Editor of Special Issues, on Fiber Optics and Passive Components (JSTQE Sept.1999), on Laser Interferometry (J. Optics A 1998 and 2002, Optical Engineering 2001), and Feature Issues of IEEE Journal Quantum Electronics, Sept. 2002, on Optical Chaos and Applications to Cryptography, and on Photodetectors (Aug. 2004). He has been a Visiting Professor at several Universities, NTU, Taipei, 2005, Sun Yat Sen (2007, 2008, 2010), and NCKU, Tainan 2012.

Michele Norgia (S'99–M'01–SM'09) was born in Omegna, Italy, in 1972. He received the M.S. degree (with Hons.) in electronics engineering from the University of Pavia, Pavia, Italy, in 1996 and the Ph.D. degree in electronics engineering and computer science in 1996. Until 2004 he was Postdoctoral Researcher in the Optoelectronics Group, the University of Pavia. In 2006, he joined the Department of Electronic and Information Science, the Politecnico di Milano as an Assistant Professor in Electronic Measurements. His main research interests include optical and electronic measurements, interferometry, chaos in lasers, optical FM standards, microelectromechanical sensors, biomedical measurements, and instrumentation. He is author of more than 150 papers published in international journals or international conference proceedings. Dr. Norgia is a member of the Italian Association "Group of Electrical and Electronic Measurements."